Polymer–Semiconductor Hybrids

Deutsche Ausgabe: DOI: 10.1002/ange.201500763
Internationale Ausgabe: DOI: 10.1002/anie.201500763

An Unconventional Route to Monodisperse and Intimately Contacted Semiconducting Organic–Inorganic Nanocomposites**

Hui Xu, Xinchang Pang, Yanjie He, Ming He, Jaehan Jung, Haiping Xia, and Zhiqun Lin**

Abstract: *We developed an unconventional route to produce uniform and intimately contacted semiconducting organic–inorganic nanocomposites for potential applications in thermoelectrics. By utilizing amphiphilic star-like PAA-b-PEDOT diblock copolymer as template, monodisperse PEDOT-functionalized lead telluride (PbTe) nanoparticles were crafted via the strong coordination interaction between PAA blocks of star-like PAA-b-PEDOT and the metal moieties of precursors (i.e., forming PEDOT–PbTe nanocomposites). As the inner PAA blocks are covalently connected to the outer PEDOT blocks, the PEDOT chains are intimately and permanently tethered on the PbTe nanoparticle surface, thereby affording a well-defined PEDOT/PbTe interface, which prevents the PbTe nanoparticles from aggregation, and more importantly promotes the long-term stability of PEDOT–PbTe nanocomposites. We envision that the template strategy is general and robust, and offers easy access to other conjugated polymer–inorganic semiconductor nanocomposites for use in a variety of applications.*

The past several decades have witnessed a rapid exploration of high-performance thermoelectric (TE) materials from the viewpoints of both scientific research and technology development. TE materials function as heat-to-electricity converters and provide an alternative route for power generation and refrigeration.[1] The grand challenge to yield TE materials with superior performance is to delicately tailor the interconnected TE physical parameters, including Seebeck coefficient S, electrical conductivity σ, and thermal conductivity κ.[2] In recent years, significant efforts have been devoted to improving the TE efficiency with different approaches, including nanostructuring,[3] doping,[4] nanocomposite formation,[5] and introduction of conducting polymers.[6] In the latter context, TE nanocomposites based on conducting polymers and inorganic nanocrystals have received increased attention as hybrid organic–inorganic nanocomposites having advantageous and attractive attributes due to their integration of the low κ of conducting polymers with the high S and σ of inorganic materials.[7] As one of the most widely studied intermediate-temperature TE system, lead telluride (PbTe)-based TE materials retain one of the highest figure of merit ZT (a measure of TE efficiency) that has ever been obtained in bulk TE materials.[8] On the other hand, it is worth noting that the best conducting polymer is poly(3,4-ethylenedioxythiophene) (PEDOT). When doped with polystyrene sulfonate (PSS), PEDOT:PSS can achieve a conductivity of up to 3000 $S\,cm^{-1}$.[9] In order to maximize the TE property, the conventional methods involve the physical mixing[10] or in situ synthesis[5d,11] of inorganic nanocrystals within PEDOT:PSS to produce hybrid organic–inorganic nanocomposites. However, it remains challenging to form a good interfacial connection between inorganic nanocrystals and conducting polymers.[12] The intimate interfacial contact between these two constituents is highly crucial as it facilitates the carrier transport without the scattering of carriers (electrons and holes) at the interface. Recently, a large number of impressive approaches, such as ligand exchange,[13] direct grafting (e.g., Heck coupling and click reaction),[14] and direct nanocrystals growth,[15] have demonstrated the feasibility of realizing the intimate contact between conducting polymers and inorganic nanocrystals (i.e., forming intimate organic–inorganic nanocomposites). However, the methods noted above usually suffer from the low long-term stability of the resulting organic–inorganic nanocomposites. The organic constituent may dissociate from inorganic counterpart or vice versa over a long period of time, as they are not connected permanently and there is a weak interaction or no strong enough binding between them. As such, this limitation would severely hinder the use of hybrid organic–inorganic nanocomposites in energy-related applications.

Herein, we report a viable and robust preparative strategy to produce spherically shaped organic–inorganic nanocomposites composed of semiconducting inorganic nanoparticles intimately and permanently tethered by conjugated polymers by utilizing rationally designed amphiphilic star-like diblock copolymers as templates. First, star-like poly(*tert*-butyl acrylate) (i.e., P*t*BA) was synthesized by atom transfer radical polymerization (ATRP) of *tert*-butyl acrylate (*t*BA) using a β-cyclodextrin-based macroinitiator. The subsequent azidation of the terminal bromines on star-like P*t*BA produced azide-functionalized P*t*BA (i.e., P*t*BA-N_3). During the synthesis of P*t*BA-N_3, in the meantime, ethynyl-terminated PEDOT (i.e., PEDOT-≡) was synthesized by a quasi-living Grignard meta-

[*] H. Xu, Prof. Dr. H. Xia
State Key Laboratory of Physical Chemistry of Solid Surfaces, College of Chemistry and Chemical Engineering
Xiamen University, Xiamen 361005 (P. R. China)
E-mail: hpxia@xmu.edu.cn

H. Xu, Dr. X. Pang, Y. He, Dr. M. He, J. Jung, Prof. Dr. Z. Lin
School of Materials Science and Engineering
Georgia Institute of Technology, Atlanta, GA 30332 (USA)
E-mail: zhiqun.lin@mse.gatech.edu

[**] This work was supported by the National Science Foundation (ECCS-1305087), the Air Force Office of Scientific Research (FA9550-13-1-0101, MURI FA9550-14-1-0037), the Minjiang Scholar Program (Z.L.), the National Natural Science Foundation of China (grant nos. 21490573 and 21174115) (H. Xia), and the China Scholarship Council (H. Xu).

Supporting information for this article is available on the WWW under http://dx.doi.org/10.1002/anie.201500763.

 © 2015 Wiley-VCH Verlag GmbH & Co. KGaA, Weinheim

thesis (GRIM) method. The rod-like PEDOT-≡ chains were then grafted onto star-like P*t*BA-N_3 by click reaction (i.e., the azide–alkyne cycloaddition) to yield star-like poly(*tert*-butyl acrylate)-*block*-poly(3,4-ethylenedioxythiophene) (i.e., star-like P*t*BA-*b*-PEDOT), which was further transformed into star-like poly(acrylic acid)-*block*-poly(3,4-ethylenedioxythiophene) (i.e., star-like PAA-*b*-PEDOT) after hydrolysis. Finally, star-like coil–rod PAA-*b*-PEDOT diblock copolymers were utilized as templates to create semiconducting organic–inorganic PEDOT–PbTe nanocomposites via the strong coordination interaction between the inner hydrophilic PAA blocks and the metal moieties of PbTe precursors. Clearly, in stark contrast to physical mixing, ligand exchange, direct grafting, and in situ synthesis of nanocrystals in the presence of conjugated polymers as in copious past work, the template strategy in this work enables the efficient synthesis of intimately contacted organic–inorganic nanocomposites in which inorganic semiconducting nanoparticles are reliably and permanently capped with semiconducting conjugated polymers. We envision that the greatly improved interfacial contact in PEDOT–PbTe nanocomposites may lead to enhanced TE efficiency when PEDOT is doped with PSS. More importantly, the amphiphilic star-like block copolymer-based template strategy can be readily extended to direct the formation a wide range of uniform, size-controllable and deterministically targeted conjugated polymer-capped semiconductor nanocrystals by controlling the molecular weight of inner hydrophilic block in amphiphilic star-like diblock copolymer and properly selecting precursors for potential applications in thermoelectrics, solar cells, sensors, among other areas.

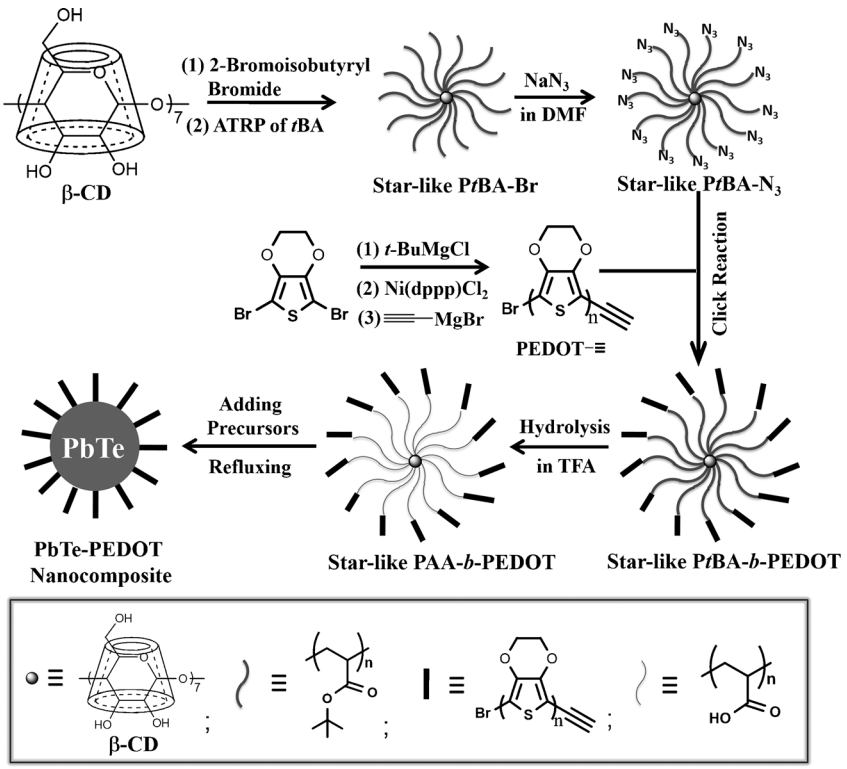

Figure 1. Formation of organic–inorganic PEDOT–PbTe nanocomposite (lower left panel) by using amphiphilic star-like PAA-*b*-PEDOT diblock copolymer (lower second panel) as template. The PEDOT–PbTe nanocomposite is composed of an inner PbTe nanoparticle (red) which is intimately and permanently capped with rod-like PEDOT chains (black). We note that only 13 PAA-*b*-PEDOT chains are shown for simplicity. As a matter of fact, 21 chains are allowed to grow from each β-CD bearing 21 hydroxy groups.

Figure 1 depicts the synthetic route to organic–inorganic nanocomposites by exploiting amphiphilic star-like coil–rod PAA-*b*-PEDOT diblock copolymer as template. The 21 hydroxy groups of β-CD were bromine-functionalized by the esterification with 2-bromoisobutyryl bromide to yield 21Br-β-CD (see Supporting Information). The latter served as macroinitiator for the atom transfer radical polymerization (ATRP) of *tert*-butyl acrylate, producing star-like P*t*BA-Br (upper second panel in Figure 1). The pure 21Br-β-CD macroinitiator and star-like P*t*BA-Br were characterized by ^{1}H NMR spectroscopy (Figures S1 and S2 in the Supporting Information). The bromine end-groups on P*t*BA-Br were substituted by azido groups to yield star-like azide-functionalized P*t*BA (i.e., P*t*BA-N_3) (upper right panel in Figure 1). The successful azidation of star-like P*t*BA-Br was confirmed by FTIR measurement. The emergence of the stretching vibration from $\nu(-N_3)$ at 2100 cm^{-1} was clearly evident in the FTIR spectrum of star-like P*t*BA-N_3 (Figure S3).

Fully undoped PEDOT has been synthesized by the dehalogenation polycondensation of the corresponding dihalomonomer in the presence of a catalytic Ni-based complex.[16] And ethynyl-terminated poly(3-hexylthiophene) has been prepared by a GRIM method.[17] On the basis of the above two approaches, we employed a modified method to synthesize PEDOT end-capped with ethynyl groups (central right panel in Figure 1). Figure S4 shows the ^{1}H NMR spectrum of ethynyl-terminated PEDOT (i.e., PEDOT-≡), signifying the successful polycondensation and alkyne functionalization. The ethynyl proton appeared at 3.48 ppm as a broad peak, and the multi-peaks between 4.15–4.40 ppm can be assigned to protons on methylene carbons. It should be noted that due to the poor solubility of PEDOT in organic solvents (e.g., THF), the molecular weight of PEDOT was low and not homogeneous, which is consistent with the report in literature.[16b] The gel-permeation chromatography (GPC) trace exhibited at least two peaks (Figure S5) and large polydispersity index for PEDOT-≡, suggesting the existence of PEDOT with different molecular weights. This correlated well with the ^{1}H NMR study in which instead of a single sharp peak, a broad peak attributed to ethynyl proton was observed. In addition, we investigated the optical absorbance of PEDOT-≡ in DMF. It is not surprising that multiple peaks located at 434 nm, 470 nm, 503 nm, and 665 nm were observed in the UV/Vis spectra of PEDOT-≡, corresponding

© 2015 Wiley-VCH Verlag GmbH & Co. KGaA, Weinheim

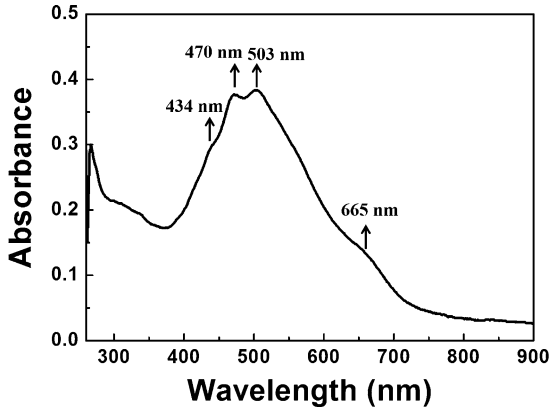

Figure 2. UV/Vis absorption spectrum of ethynyl-teminated PEDOT (PEDOT-≡) in *N*,*N*-dimethylformamide (DMF).

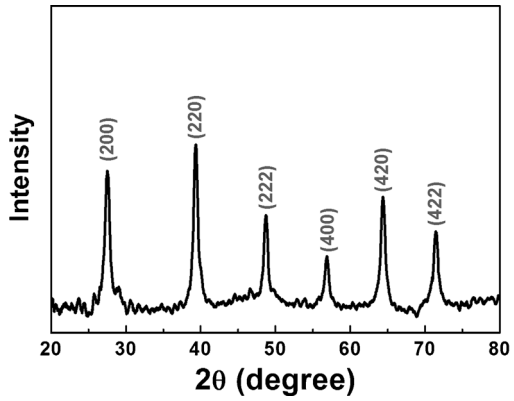

Figure 3. XRD pattern of PEDOT-capped PbTe nanoparticles.

to different molecular weights of PEDOT presented in the system (Figure 2).[16b] Based on the calculation from the ^{1}H NMR spectrum, the average molecular weight of PEDOT-≡ was found to be approximately 1100 g mol^{-1}, indicating that the product was essentially composed of oligomers.

The successful synthesis of star-like P*t*BA-*b*-PEDOT diblock copolymer by click reaction between star-like P*t*BA-N_3 and PEDOT-≡ (i.e., the azide–alkyne cycloaddition; lower right panel in Figure 1) was corroborated by ^{1}H NMR and GPC characterizations. The signal associated with the triazole ring at $\delta = 7.75$–8.00 ppm appeared in star-like P*t*BA-*b*-PEDOT diblock copolymer (Figure S6). The broad peak at $\delta = 4.19$–4.41 ppm corresponds to the methylene protons of PEDOT, and the high-field signal at $\delta = 1.0$–2.5 ppm can be assigned to protons of P*t*BA. Notably, after the click reaction, the molecular weight of P*t*BA-*b*-PEDOT increased as measured by GPC (Figure S7). Table S1 summarizes the structural parameters of star-like P*t*BA-Br and P*t*BA-*b*-PEDOT synthesized in this work. Finally, the hydrolysis of inner P*t*BA blocks with trifluoroacetic acid yielded amphiphilic star-like PAA-*b*-PEDOT diblock copolymer containing inner hydrophilic PAA blocks and outer hydrophobic PEDOT blocks (lower second panel in Figure 1; see Supporting Information).

By subjecting the PbTe precursors to react with amphiphilic star-like PAA-*b*-PEDOT, high-quality organic–inorganic PEDOT–PbTe nanocomposite composed of uniform semiconducting PbTe nanoparticles with conjugated PEDOT chains intimately and permanently situated on its surface were crafted (i.e., PEDOT-capped PbTe nanoparticle; lower left panel in Figure 1; see Supporting Information). The amphiphilic star-like PAA-*b*-PEDOT served as template and directed the formation of PbTe nanoparticle via the preferential coordination interaction between −COOH groups of PAA blocks and the metal moieties of PbTe precursors. A representative X-ray diffraction (XRD) profile of the resulting PEDOT–PbTe nanocomposites is shown in Figure 3. The characteristic peaks can be indexed to pure face-centered cubic phase of PbTe, in good agreement with the standard XRD profile of bulk PbTe. We note that the broadening of peaks can be ascribed to the finite size of PbTe nanoparticles. Moreover, as the mixture solution was refluxed under Ar at 160 °C for 4 h, the very broad XRD peak of PEDOT located at $2\theta = 20$–$25°$ was rather weak, which is in good agreement with the report in literature.[18]

Transmission electron microscopy (TEM) imaging was also performed to examine the morphology and size of as-prepared PEDOT-capped PbTe nanoparticles. Strikingly, highly spherical PbTe nanoparticles with an average diameter of 10.8 ± 0.5 nm were formed, as revealed by TEM imaging (Figure 4). A histogram of the size distribution of synthesized nanoparticles was depicted in Figure S8. As their size distribution lies within 5% of the average size, they are monodisperse. Such remarkable uniformity of PbTe nanoparticles was a direct consequence of the narrow molecular weight distribution of P*t*BA blocks (i.e., low PDI in Table S1; hydrolyzed into PAA later for reacting with the precursors) in star-like P*t*BA-*b*-PEDOT. As star-like P*t*BA was synthesized

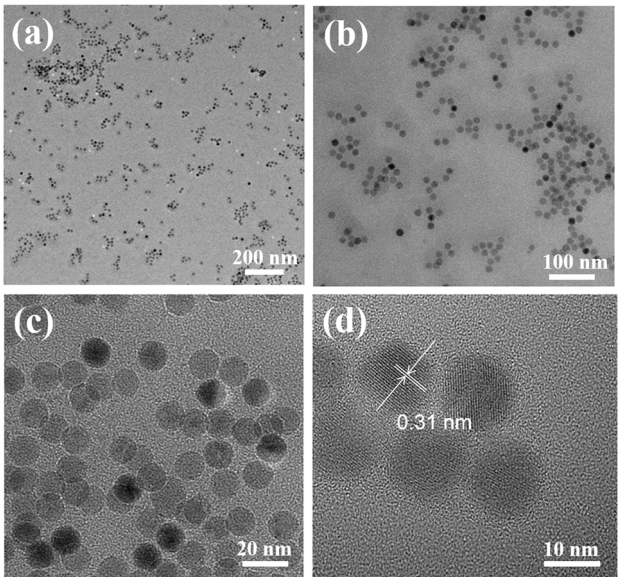

Figure 4. TEM images of monodisperse PEDOT-capped PbTe nanoparticles prepared by using amphiphilic star-like PAA-*b*-PEDOT as template. The average diameter of PEDOT-capped PbTe nanoparticles was 10.8 ± 0.5 nm. Scale bars are 200 nm in (a), 100 nm in (b), 20 nm in (c), and 10 nm in (d) where the crystalline lattices are clearly evident.

© 2015 Wiley-VCH Verlag GmbH & Co. KGaA, Weinheim

by ATRP, a living polymerization technique, each P*t*BA possessed well-defined chain length, thereby templating the formation of monodisperse PbTe nanoparticles after transforming P*t*BA blocks into PAA blocks. The high-resolution TEM (HRTEM) image of PbTe nanoparticles clearly showed that the nanoparticle was highly crystalline with a lattice-fringe distance of ca. 3.1 Å, which is in good correlation with the (200) interplanar distance of 3.2 Å of the face-centered cubic PbTe (Figure 4d). It is worth noting that the PEDOT chains anchored on the surface of PbTe nanoparticle was not observed under TEM likely due to their low electron density compared to inorganic PbTe nanocrystal and the short chain length of PEDOT (average molecular weight of 1100 $g\,mol^{-1}$ as described above).

Energy dispersive X-ray spectroscopy (EDS) analysis (Figure S9) was also performed on intimately contacted PEDOT–PbTe nanocomposites to confirm the chemical composition. An atomic ratio of Pb:Te = 1:1 was found, further substantiating the formation of PbTe. It is interesting to note that, although PEDOT chains cannot be identified by TEM as noted above, the element sulfur in PEDOT was clearly detected by the EDS measurement. In addition to the ^{1}H NMR and GPC studies proving the success in grafting PEDOT chains on star-like PAA, this piece of information further suggested the presence of the PEDOT capping on the PbTe nanoparticle surface.

In the following we turned our attention to the formation mechanism of PbTe nanoparticles (Figure S10). First, NaHTe is produced from tellurium powder using $NaBH_4$ as a reducing agent (reaction (1)). Subsequently, $Pb(NO_3)_2$ is added to the NaHTe solution under the alkaline conditions, yielding the Pb(HTe)(OH) complex (reaction (2)). Finally, in the formation of uniform spherical PbTe nanoparticles, the PAA-*b*-PEDOT template plays a key role in controlling the nucleation and growth of PbTe nanocrystals. The inner PAA blocks in star-like PAA-*b*-PEDOT diblock copolymer are highly hydrophilic,[19] facilitating the selective incorporation of precursors into the interior space occupied by PAA blocks through strong coordination interaction between the Pb(HTe)(OH) complex and the −COOH groups of PAA. Rapid reaction of lead complex in reaction (3) results in PbTe nanoparticles through dehydration at high temperature (Figure S10), as unambiguously evidenced by TEM imaging.

In summary, we demonstrated an unconventional and robust template strategy for crafting monodisperse conjugated polymer-capped semiconductor nanoparticles (i.e., PEDOT-capped PbTe nanoparticles). Conjugated polymers and semiconductor nanoparticle were inextricably contacted (i.e., forming intimately contacted PEDOT–PbTe nanocomposites) by exploiting the rationally designed amphiphilic star-like coil–rod PAA-*b*-PEDOT diblock copolymer as template. The PEDOT–PbTe nanocomposites is characterized by well-defined organic–inorganic interface, which prevents the PbTe nanoparticles from aggregation, and more importantly enables the long-term stability of nanocomposites due to the presence of permanently tethered PEDOT chains on the surface of PbTe nanoparticle. As such, these nanocomposites are particularly promising for use in organic–inorganic hybrid thermoelectrics with improved TE efficiency after doping PEDOT with PSS, as the intimate contact between PEDOT:PSS and PbTe would promote the carrier transport by eliminating the scattering of carriers at the interface. The mixing of PEDOT in PEDOT–PbTe nanocomposites with PSS would afford water-soluble PEDOT:PSS–PbTe nanocomposites. This merits a detailed study and will be the subject of our future work. We also envision that the template strategy developed in this work is general and can be immediately extended to construct an exciting variety of intriguing intimately contacted organic–inorganic nanocomposites with diversified and complex structures and compositions when the precursors are properly chosen for promising applications in thermoelectrics, optics, optoelectronics, sensors, energy conversion and storage, etc.

Keywords: lead telluride · organic–inorganic nanocomposites · PEDOT · polymer template · thermoelectrics

How to cite: *Angew. Chem. Int. Ed.* **2015**, *54*, 4636–4640
Angew. Chem. **2015**, *127*, 4719–4723

[1] a) J. Yang, T. Caillat, *MRS Bull.* **2006**, *31*, 224–229; b) M. He, F. Qiu, Z. Lin, *Energy Environ. Sci.* **2013**, *6*, 1352–1361.
[2] G. J. Snyder, E. S. Toberer, *Nat. Mater.* **2008**, *7*, 105–114.
[3] a) R. Venkatasubramanian, E. Siivola, T. Colpitts, B. O'Quinn, *Nature* **2001**, *413*, 597–602; b) T. C. Harman, P. J. Taylor, M. P. Walsh, B. E. LaForge, *Science* **2002**, *297*, 2229–2232; c) B. Poudel, Q. Hao, Y. Ma, Y. C. Lan, A. Minnich, B. Yu, X. A. Yan, D. Z. Wang, A. Muto, D. Vashaee, X. Y. Chen, J. M. Liu, M. S. Dresselhaus, G. Chen, Z. F. Ren, *Science* **2008**, *320*, 634–638.
[4] a) G. H. Kim, L. Shao, K. Zhang, K. P. Pipe, *Nat. Mater.* **2013**, *12*, 719–723; b) Q. Zhang, H. Wang, Q. Zhang, W. S. Liu, B. Yu, H. Wang, D. Wang, G. Ni, G. Chen, Z. Ren, *Nano Lett.* **2012**, *12*, 2324–2330; c) A. D. LaLonde, Y. Pei, G. J. Snyder, *Energy Environ. Sci.* **2011**, *4*, 2090–2096.
[5] a) C. Meng, C. Liu, S. Fan, *Adv. Mater.* **2010**, *22*, 535–539; b) N. Toshima, M. Imai, S. Ichikawa, *J. Electron. Mater.* **2011**, *40*, 898–902; c) E. Pintér, Z. A. Fekete, O. Berkesi, P. Makra, A. Patzko, C. Visy, *J. Phys. Chem. C* **2007**, *111*, 11872–11878; d) Y. Wang, K. Cai, X. Yao, *ACS Appl. Mater. Interfaces* **2011**, *3*, 1163–1166; e) D. Kim, Y. Kim, K. Choi, J. C. Grunlan, C. H. Yu, *Acs Nano* **2010**, *4*, 513–523.
[6] a) A. B. Kaiser, *Adv. Mater.* **2001**, *13*, 927–941; b) L. Yan, M. Shao, H. Wang, D. Dudis, A. Urbas, B. Hu, *Adv. Mater.* **2011**, *23*, 4120–4124; c) O. Bubnova, Z. U. Khan, A. Malti, S. Braun, M. Fahlman, M. Berggren, X. Crispin, *Nat. Mater.* **2011**, *10*, 429–433; d) M. Leclerc, A. Najari, *Nat. Mater.* **2011**, *10*, 409–410.
[7] Y. Du, S. Z. Shen, K. Cai, P. S. Casey, *Prog. Polym. Sci.* **2012**, *37*, 820–841.
[8] a) K. Biswas, J. Q. He, Q. C. Zhang, G. Y. Wang, C. Uher, V. P. Dravid, M. G. Kanatzidis, *Nat. Chem.* **2011**, *3*, 160–166; b) K. F. Hsu, S. Loo, F. Guo, W. Chen, J. S. Dyck, C. Uher, T. Hogan, E. K. Polychroniadis, M. G. Kanatzidis, *Science* **2004**, *303*, 818–821.
[9] Y. Xia, K. Sun, J. Ouyang, *Adv. Mater.* **2012**, *24*, 2436–2440.
[10] a) C. C. Liu, F. X. Jiang, M. Y. Huang, B. Y. Lu, R. R. Yue, J. K. Xu, *J. Electron. Mater.* **2011**, *40*, 948–952; b) B. Zhang, J. Sun, H. E. Katz, F. Fang, R. L. Opila, *ACS Appl. Mater. Interfaces* **2010**, *2*, 3170–3178.
[11] a) K. C. See, J. P. Feser, C. E. Chen, A. Majumdar, J. J. Urban, R. A. Segalman, *Nano Lett.* **2010**, *10*, 4664–4667; b) S. K. Yee, N. E. Coates, A. Majumdar, J. J. Urban, R. A. Segalman, *Phys. Chem. Chem. Phys.* **2013**, *15*, 4024–4032.

 © 2015 Wiley-VCH Verlag GmbH & Co. KGaA, Weinheim

[12] a) M. He, J. Ge, Z. Lin, X. Feng, X. Wang, H. Lu, Y. Yang, F. Qiu, *Energy Environ. Sci.* **2012**, *5*, 8351 – 8358; b) L. Zhao, Z. Q. Lin, *Adv. Mater.* **2012**, *24*, 4353 – 4368; c) J. Jung, Y. J. Yoon, M. He, Z. Lin, *J. Polym. Sci. Part B* **2014**, *52*, 1641 – 1660; d) M. He, F. Qiu, Z. Lin, *J. Phys. Chem. Lett.* **2013**, *4*, 1788 – 1796.

[13] a) D. J. Milliron, A. P. Alivisatos, C. Pitois, C. Edder, J. M. J. Frechet, *Adv. Mater.* **2003**, *15*, 58 – 61; b) J. Liu, T. Tanaka, K. Sivula, A. P. Alivisatos, J. M. J. Frechet, *J. Am. Chem. Soc.* **2004**, *126*, 6550 – 6551; c) N. A. Frey, S. Peng, K. Cheng, S. H. Sun, *Chem. Soc. Rev.* **2009**, *38*, 2532 – 2542.

[14] a) J. Xu, J. Wang, M. Mitchell, P. Mukherjee, M. Jeffries-El, J. W. Petrich, Z. Lin, *J. Am. Chem. Soc.* **2007**, *129*, 12828 – 12833; b) L. Zhao, X. Pang, R. Adhikary, J. W. Petrich, Z. Lin, *Angew. Chem. Int. Ed.* **2011**, *50*, 3958 – 3962; *Angew. Chem.* **2011**, *123*, 4044 – 4048; c) L. Zhao, X. Pang, R. Adhikary, J. W. Petrich, M. Jeffries-EL, Z. Lin, *Adv. Mater.* **2011**, *23*, 2844 – 2849.

[15] a) A. Watt, E. Thomsen, P. Meredith, H. Rubinsztein-Dunlop, *Chem. Commun.* **2004**, 2334 – 2335; b) A. Stavrinadis, R. Beal, J. M. Smith, H. E. Assender, A. A. R. Watt, *Adv. Mater.* **2008**, *20*, 3105 – 3109.

[16] a) T. Yamamoto, M. Abla, *Synth. Met.* **1999**, *100*, 237 – 239; b) F. Tran-Van, S. Garreau, G. Louarn, G. Froyer, C. Chevrot, *J. Mater. Chem.* **2001**, *11*, 1378 – 1382.

[17] M. Jeffries-El, G. Sauve, R. D. McCullough, *Macromolecules* **2005**, *38*, 10346 – 10352.

[18] Z. A. King, C. M. Shaw, S. A. Spanninga, D. C. Martin, *Polymer* **2011**, *52*, 1302 – 1308.

[19] X. Pang, L. Zhao, W. Han, X. Xin, Z. Lin, *Nat. Nanotechnol.* **2013**, *8*, 426 – 431.

Received: January 26, 2015
Published online: February 25, 2015

 © 2015 Wiley-VCH Verlag GmbH & Co. KGaA, Weinheim